

Output Voltage Control using Primary-Side Parameter Estimation Method for WPT System

Supakorn Luemkham¹, Praewa Hariruk¹, Krittisak Klangnet¹, Hatta Sawachan¹ and Kan Voottipruex^{1*}

¹Department of Electrical Engineering Technology, College of Industrial Technology, King Mongkut's University of Technology North Bangkok, Bangkok, Thailand, hatta.s@cit.kmutnb.ac.th kan.v@cit.kmutnb.ac.th*

Abstract

This paper proposes an output voltage control method for Wireless Power Transfer (WPT) systems that uses primary-side parameter estimation, eliminating the need for wireless communication between the primary and secondary sides. Conventional closed-loop control methods typically rely on a dedicated wireless communication channel to send feedback from the secondary side, which adds cost, complexity, and potential reliability issues. The proposed method overcomes these drawbacks by implementing a primaryside controller that analyzes the primary-side voltage and current waveforms to accurately estimate the output voltage. This estimation allows for the direct calculation and precise regulation of the output voltage across varying load conditions. Experimental results validate the proposed system, demonstrating stable output voltage and high efficiency.

Keywords: Output voltage control, Parameter estimation method, Wireless power transfer.

1. General Information

Wireless power transfer (WPT) systems are used in charging applications such as biomedical implants [1], mining applications [2], underwater applications [3], and electric vehicles (EVs) [4]. The ability to transfer power across an air gap without physical connectors enhances safety, durability, and user experience. Among the various WPT topologies, inductively coupled power transfer (IPT) systems are widely adopted due to their high efficiency and power capability [5]. The compensation topology in a WPT system is normally applied minimize the VA rating and maximizing the power transfer efficiency of the loosely coupled coils.

In wireless power transfer systems, there are four basic compensation topologies: Series-Series (SS), Series-Parallel (SP), Parallel-Series (PS), and Parallel-Parallel (PP) [5]. The Series-Series (SS) compensation topology is widely used due to its high power efficiency and purely resistive reflected impedance. A critical challenge in the practical implementation of SS topology in WPT systems is regulating the output voltage on the secondary side, as it is highly sensitive to variations in load resistance. However, applying an SS topology in a WPT system at its resonant frequency results in a constant current output [5]. Consequently, the output voltage varies directly with the load, making it difficult to regulate. To maintain a constant output voltage, conventional systems typically require an additional DC-DC converter on the secondary side, complex control schemes, and wireless communication between the primary and secondary sides [6] as shown in Figure 1. Nevertheless, achieving stable voltage regulation across a wide range of load variations remains a significant challenge.

This paper proposes an output voltage control method for WPT systems that uses a primary-side controller, eliminating the need for secondary-to-primary communication. The controller analyzes primary-side voltage and current waveforms to accurately estimate the output voltage. This enables the direct calculation and precise regulation of the output voltage across a wide range of operating load conditions. This paper is organized as follows: Section 2 presents an analysis of the design parameters for the SS topology, Section 3 describes the details of the coil design, Section 4 presents the proposed WPT system, and Section 5 provides experimental results to validate the system's performance.

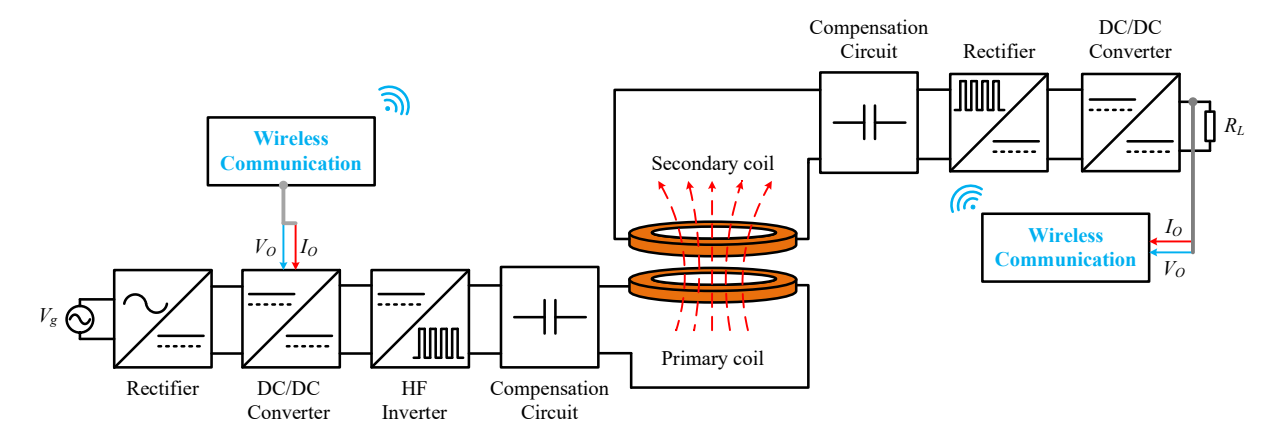


Fig. 1 Conventional WPT system

2. Analysis of SS Topology

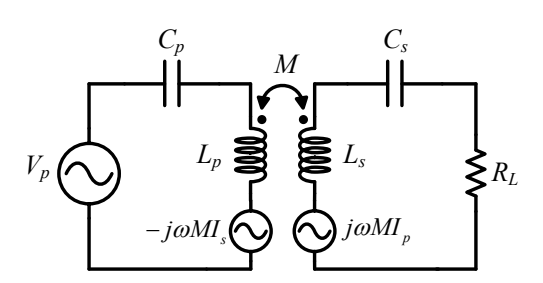


Fig. 2 Equivalent of SS topology

The equivalent circuit of the series–series compensated circuit (SS topology) is shown in Figure 2. The circuit consists of the primary side and the secondary side. On the primary side, the primary voltage (V_p) is connected in series with the primary capacitor (C_p) and the primary coil (L_p) . The primary impedance can be calculated by

$$Z_p = j\omega L_p + \frac{1}{j\omega C_p} \tag{1}$$

On the secondary side, the secondary coil (L_s) is connected in series with the secondary capacitor (C_s) and the load (R_L) . The secondary impedance can be calculated by

$$Z_s = j\omega L_s + \frac{1}{j\omega C} + R_L \tag{2}$$

Both sides of the circuit are magnetically coupled. The impedance of the secondary side is reflected to the primary side through the mutual inductance (M). The reflected impedance can be expressed by

$$Z_r = -j\omega M I_s = \frac{\omega^2 M^2}{Z}$$
 (3)

Therefore, the input impedance (Z_{in}) can be calculated by

$$Z_{in} = \text{Re}(Z_{in}) + \text{Im}(Z_{in}) = Z_n + Z_r$$
 (4)

A WPT system is typically designed to operate at the same resonant frequency (ω_0) on both sides. This causes the input reactance to become zero, enhancing power transfer capability and minimizing the supply's apparent power (VA) rating. The resonant frequency can be expressed by

$$\omega_0 = \frac{1}{\sqrt{L_p C_p}} = \frac{1}{\sqrt{L_s C_s}} \tag{5}$$



The SS topology provides a load-independent output current characteristic at the resonant frequency (ω_0) . The amplitude of the secondary current (I_s) in terms of the primary voltage (V_p) at the resonant frequency which can be expressed by

$$\left|I_{s}\right|_{\omega=\omega_{0}} = \frac{V_{p}}{\omega_{0}M} \tag{6}$$

The secondary voltage (V_s) at the resonant frequency can be calculated by

$$V_{s} = j\omega_{0}MI_{p} \tag{7}$$

However, the amplitude of the secondary voltage (V_s) in terms of the primary voltage (V_p) at the resonant frequency depends on load, which can be expressed as

$$\left|V_{s}\right|_{\omega=\omega_{0}} = \frac{R_{L}V_{p}}{\omega_{0}M} \tag{8}$$

Therefore, this paper presents a method for estimating the secondary-side voltage using mathematical approximation based on primary-side parameters, with the obtained value used to control the output voltage. The parameter estimation method will be presented in Section 4.

3. Coil Design

A circular coil was selected for its simplicity and symmetrical shape. The coil parameters are listed in Table 1, and the coil prototypes are shown in Figure 3. The dimensions are designed to suit low-power applications, such as mobile robotics, with a 5 cm air-gap.

Table 1 Parameters of coils

Parameters	Values	Unit
Inner radius	5	cm
Outer radius	15	cm
Coil inductance: L_p	74.16	μΗ
Coil inductance: L_s	73.74	μΗ
Mutual inductance	21.24	μΗ





Fig. 3 Coil prototype



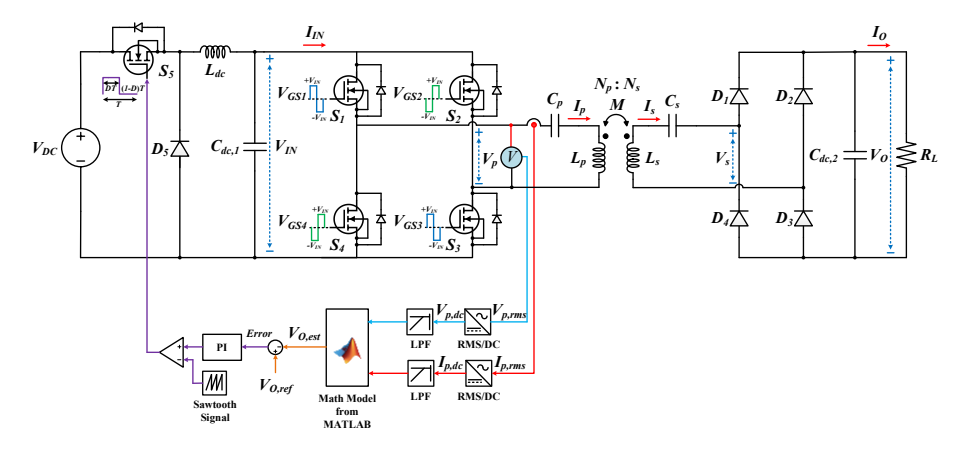


Fig. 4 Proposed WPT system

4. Proposed WPT System

The proposed WPT system is a composite of the primary side and secondary side. The primary side includes a buck converter, a full-bridge inverter, a primary capacitor, and a primary coil. The secondary side includes a secondary coil, a secondary capacitor, a bridge diode rectifier, a capacitive output filter, and load. The schematic of the proposed WPT system is shown in Figure 4 and the electrical parameters listed in Table 2. A DC input voltage of 48 volts is supplied to a buck converter, which operates at a switching frequency of 25 kHz. The buck converter controls the amplitude of the voltage supplied to the inverter. The inverter then converts the DC voltage obtained from the buck converter into a high-frequency square-wave voltage. The fixedfrequency control was adopted in the paper to provide a the resonant frequency ($f_0 = 85 \text{ kHz}$).

The method for estimating the secondary-side voltage, based on the secondary-side voltage equation at the resonant frequency in (8), can be performed by approximating the load resistance from the primary-side parameters, which can be estimated by

$$R_{L,est} = \left(\frac{\omega_0^2 M^2 I_p}{V_p}\right) \tag{9}$$

Therefore, the secondary voltage can be approximated using a primary-side parameter estimation method that includes the primary voltage, primary current, and estimated load resistance, which can be calculated by

$$\left| V_{s,est} \right|_{\omega = \omega_0} = \sqrt{V_p I_p R_{L,est}} \tag{10}$$

The square waveform of the secondary voltage can be described as,

$$V_{s,est}(t) = \frac{4V_m}{\pi} \sum_{n} \frac{1}{n} \sin(n\omega_0 t)$$
 (11)

where i = 1, 2, 3, ..., n.

Table 2 Electrical parameters for the proposed WPT system

Parameters	Values	Unit
Inverter frequency (f_{inv})	85	kHz
Buck converter frequency (f_{buck})	25	kHz
DC input voltage (V_{DC})	48	V
Primary coil inductance (L_p)	74.16	μН
Secondary coil inductance (L_s)	73.74	μΗ
Primary capacitance (C_p)	46.81	nF
Secondary capacitance (C_s)	46.94	nF
Mutual inductance (M)	21.24	μН

Therefore, the output voltage across the bridge rectifier with a capacitive output filter can be estimated by,

$$\left|V_{O,est}\right|_{\omega=\omega_0} = \left|V_{s,est}\right|_{\omega=\omega_0} - 2V_F \tag{12}$$

where V_F is forward voltage of bridge diode.

The estimation of output voltage in (12) was calculated in the microcontroller unit and used as feedback for PI controller. Hence, the output voltage can be controlled by a buck converter on the primary side as illustrated in Figure 4.

5. Experiment

A hardware prototype with a 11 Ω load resistance was constructed to verify the proposed method, as shown in Figure 5.

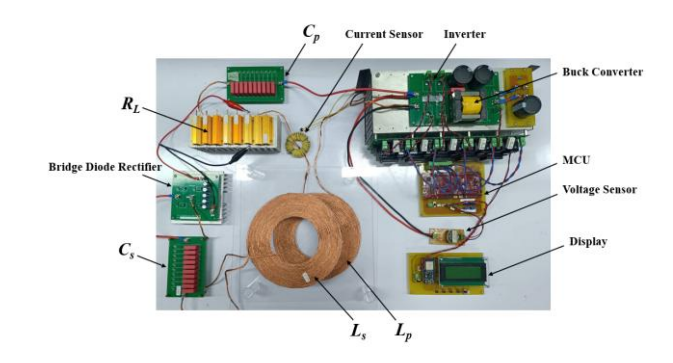


Fig. 5 Hardware prototype

The 48th Electrical Engineering Conference (EECON-48)

วันที่ 19-21 พฤศจิกายน 2568 ณ โรงแรมฟูราม่า จังหวัดเชียงใหม่

The experimental results indicated a DC input voltage (V_{DC}) of 47.3 V and an input current (I_{DC}) of 1.42 A, as illustrated in Figure 6. Correspondingly, Figure 7 shows a primary voltage (V_p) of 33.2 V with a primary current (I_p) of 2.52 A, and a secondary voltage (V_s) of 27.7 V with a secondary current (I_s) of 2.63 A. Finally, the results in Figure 8 illustrate an output voltage (V_O) of 24.5 V and an output current (I_O) of 2.32 A.

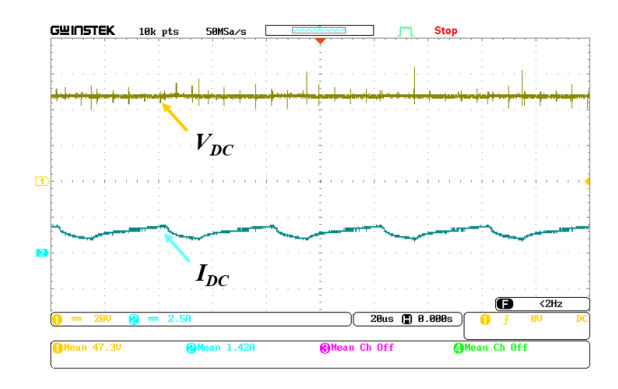


Fig. 6 Experimental waveforms of V_{DC} and I_{DC}

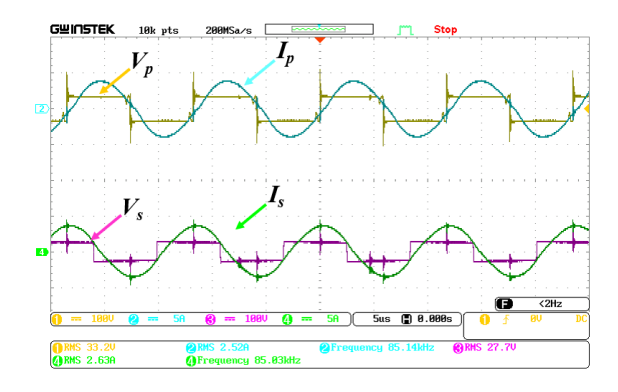


Fig. 7 Experimental waveforms of Vp, Ip, Vs, and Is

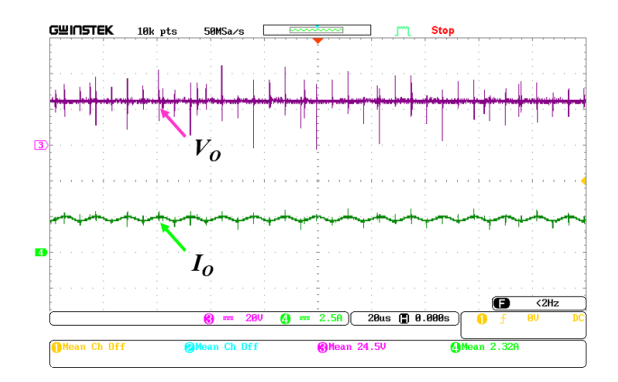


Fig. 8 Experimental waveforms of V_O and I_O



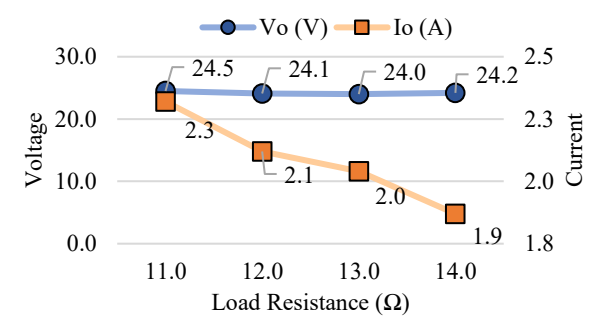


Fig. 9 Output voltage and output current versus different load resistances

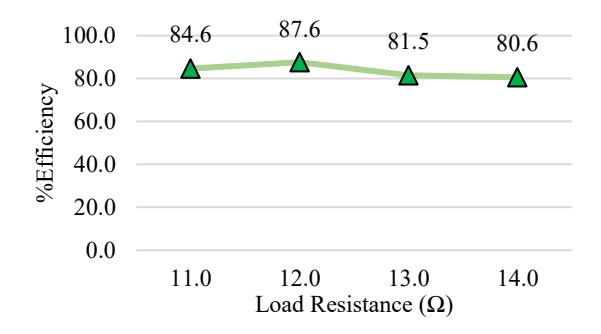


Fig. 10 Experimental Efficiency versus load resistances

Subsequently, varying load resistance was set up in the experiment to demonstrates constant output voltage behavior. The graph in Figure 9 illustrates the relationship between load resistance, output voltage (V_o), and output current (I_o). As the load resistance was increased from 11 Ω to 14 Ω , the output voltage (blue line) remained highly stable, fluctuating minimally between 24.2 V and 24.5 V. In contrast, the output current (orange line) showed a clear inverse relationship with resistance, decreasing steadily from a maximum of 2.3 A at 11 Ω to a minimum of 1.9 A at 14 Ω .

Figure 10 shows the system's efficiency as a function of varying load resistance from 11 Ω to 14 Ω . Efficiency initially increases with resistance, rising from 84.6% at 11 Ω to a peak of 87.6% when the load resistance is 12 Ω . Beyond this optimal point, efficiency continues to drop, reaching 81.5% at 13 Ω and 80.6% at 14 Ω . This trend demonstrates that the system achieves its maximum operational efficiency at a specific load resistance of 12 Ω .

6. Conclusions

This paper validates a primary-side control method for a Series-Series (SS) Wireless Power Transfer (WPT) system that eliminates the need for a secondary wireless communication. The controller accurately regulates the output voltage by estimating it from primary-side voltage and current measurements. A hardware prototype confirmed the method's effectiveness, maintaining a stable at 24 V ($\pm 2\%$) output under varying loads (11 to 14 Ω) while achieving a maximum efficiency of 87.6%.

วันที่ 19-21 พฤศจิกายน 2568 ณ โรงแรมฟูราม่า จังหวัดเชียงใหม่

References

- [1] P. Si, A. P. Hu, S. Malpas, and D. Budgett, "A frequency control method for regulating wireless power to implantable devices," *IEEE Trans. Biomed. Circuits Syst.*, vol. 2, pp. 22-29, 2008.
- [2] K. W. Klontz, D. M. Divan, D. W. Novotny, and R. D. Lorenz, "Contactless power delivery system for mining applications," *IEEE Trans. Ind. Applicat.*, vol. 31, pp. 27-35, 1995.
- [3] J. Kuipers, H. Bruning, S. Bakker, and H. Rijnaarts, "Near field resonant inductive coupling to power electronic devices dispersed in water," *Sens. Actuators A Phys.*, vol. 178, pp. 217-222, 2012.
- [4] S. Hasanzadeh, S. Vaez-Zadeh, and A. H. Isfahani, "Optimization of a contactless power transfer system for electric vehicles," *IEEE Trans. Veh. Technol.*, vol. 61, pp. 3566-3573, 2012.
- [5] V. Shevchenko, O. Husev, R. Strzelecki, B. Pakhaliuk, N. Poliakov, and N. Strzelecka, "Compensation topologies in IPT systems: standards, requirements, classification, analysis, comparison and application," *IEEE Access*, vol. 7, pp. 120559-120580, 2019.
- [6] T. Diekhans, and R. W. De Doncker, "A dual-side controlled inductive power transfer system optimized for large coupling factor variations and partial load," *IEEE Trans. Power Electron.*, vol. 30, pp. 6320-6328, 2015.



Supakorn Luemkham: graduated with a vocational certificate in the field of Electrical Power Engineering in 2021 and an advanced vocational certificate in the field of Electrical Power Engineering in 2023. He is currently studying for a

Bachelor of Industrial Technology in Electrical and Power Electronics Technology, Department of Electrical Engineering Technology, College of Industrial Technology, King Mongkut's University of Technology North Bangkok (KMUTNB).



Praewa Hariruk: graduated with a vocational certificate in Power Electronics in 2021 and an advanced vocational certificate in Power Electricity in 2023 from Phranakhon Si Ayutthaya Technical College. She is currently

studying for a Bachelor of Industrial Technology in Electrical and Power Electronics Technology, Department of Electrical Engineering Technology, College of Industrial Technology, King Mongkut's University of Technology North Bangkok (KMUTNB).





Krittisak Klangnet: graduated with vocational certificate in Electrical Power in 2020 and advanced vocational certificate in Electrical Control in 2022. He is currently studying for a Bachelor of Industrial Technology in Electrical and

Power Electronics Technology, Department of Electrical Engineering Technology, College of Industrial Technology, King Mongkut's University of Technology North Bangkok (KMUTNB).



Hatta Sawachan: received the B.Ind.Tech. degree in Power Electronics Technology from King Mongkut's University of Technology North Bangkok (KMUTNB), Bangkok, Thailand, in 2014, and the M.Eng. degree in Electrical

Engineering (Automatic Control) from the same university in 2017. He is currently an Assistant Professor with the Department of Electrical Engineering Technology, College of Industrial Technology, KMUTNB. His research interests include Power Electronics (Power Converter, Grid Connection, Electric Drive), Control System, and Digital Control.



Kan Voottipruex: received the B.Eng. degree in Electronic and Telecommunication Engineering from King Mongkut's University of Technology Thonburi (KMUTT), Bangkok, in 2014, and the M.Eng. degree

in Electrical Engineering from King Mongkut's University of Technology Thonburi (KMUTT), Bangkok, in 2017. He is currently a lecturer with the Department of Electrical Engineering Technology, College of Industrial Technology, King Mongkut's University of Technology North Bangkok (KMUTNB). His research interests include inductive power transfer systems (IPT), wireless charging applications, and renewable energy applications.